Proceedings of the ASME 2013 Dynamic Systems and Control Conference
DSCC2013
October 21-23, 2013, Palo Alto, California, USA

DSCC2013-3840

AN APPLICATION OF THE AUTOGYRO THEORY TO AIRBORNE WIND ENERGY EXTRACTION

Sigitas Rimkus, Tuhin Das *
Mechanical and Aerospace Engineering Department
University of Central Florida
Orlando, Florida 32816
Email: Tuhin.Das@ucf.edu

ABSTRACT

Auto-rotation or autogyro is a well-known phenomenon where a rotor in a wind field generates significant lift while the wind induces considerable aerodynamic torque on the rotor. The principle has been studied extensively for applications in aviation. However, with recent works indicating immense, persistent, and pervasive, available wind energy at high altitudes, the principle of autogyro could potentially be exploited for energy harvesting. In this paper, we carry out a preliminary investigation on the viability of using autogyros for energy extraction. We mainly focus on one of the earliest documented works on modeling of autogyro and extend its use to explore energy harvesting. The model is based on blade element theory. We provide simulation results of the concept. Although the results are encouraging, there are various practical aspects that need to be investigated to build confidence on this approach of energy harvesting. This work aims to build a framework upon which more comprehensive research can be conducted.

NOMENCLATURE

B Number of blades
c Blade chord
H Longitudinal force
k_L, k_D Lift and drag coefficients of blade element
Q Aerodynamic Torque
R Blade radius
T Thrust force
V Velocity of aircraft/wind
W Total weight
X Effective drag force
Y Lateral force
Z Effective lift force
α Blade pitch angle
β Angular rotation of blade about hinge
β_0, β_1, ϕ_1 Fourier series parameters of flapping motion
θ Angle of incidence of autogyro
λ Tip speed ratio
μ Axial flow ratio
ρ Density of air
σ Blade solidity
ψ Angular position of blade
Ω Angular velocity about shaft

BACKGROUND AND INTRODUCTION

Wind data from high altitudes shows that there is an abundance of wind power available and that its availability isn't restricted by geographical location. A study in [1] provides an insight to the magnitude of wind power available at altitudes of 7-16km, which is roughly 100 times that of the global energy demand. This abundance of energy is primarily attributed to the existence of jet streams [2]. It has prompted a renewed interest in airborne wind energy (AWE) systems.

Airborne wind energy devices in the form of airborne windmills were first proposed in the first half of the 1900s. Originally conceived to power communications aerostats, windmills were placed on the aircraft and were used to generate the power needed to run the communications equipment [3]. The concept of a rotorcraft placed permanently in the upper atmosphere was proposed by Fletcher [4]; the rotors were designed to generate electricity as well as provide lift to support the airframe. Stability analysis of the proposed system showed the need for an active

*Address all correspondence to this author.

control mechanism in order to maintain flight.

In recent years, alternative energy research has attracted attention and with it there has been a renewal of interest in airborne wind energy. Ockels [5] proposed the Laddermill concept; a device comprised of a series of kites that move a closed cable through a generator. Several variations on the Laddermill concept also exist in literature [6–8]. Current AWE device designs can be classified according to [9]:

Altitude

1. Low and medium
2. >600m above ground

Generator Position

1. On ground
2. On board

Device Weight

1. Lighter than air (LTA)
2. Heavier than air (HTA)

Aerodynamics

1. Helicopter type
2. Airfoil type (kite, wing, etc.)
3. Aerostat type

In all these categories, most of recent and ongoing research are essentially in low and medium altitude range (typically less than 1km). However, jet streams occur at much higher altitudes (10-12kms).

In prior work [10, 11], we proposed using tethered airfoils to tap into the energy available in the wind at high altitudes. However, for high altitudes, the proposed method of generating power by reeling the kite in and out from a base point, or by using a moving base to harvest energy appear impractical. At 10-12km tether lengths needed to access higher altitudes, a reeling action or a mobile base would be subject to large time delays and uncertainties between the base and the kite which would result in numerous issues from a control and stability standpoint. Instead, we propose replacing the tethered airfoil with a tethered autogyro device. In [2] the authors discussed a power generator based on the concept of the autogyro, however a thorough mathematical analysis is lacking in this work. The objective of this work is to build a mathematical model of the autogyro based on first principles. In this regard, we revisit the theory of the autogyro that was first formally developed in the mid-1920s [12, 13] and then expanded upon in the mid-1930s [14]. In principle, an autogyro, also called a gyroplane, uses an unpowered rotor in a state of autorotation to develop lift. Autorotation is a flight state where the rotor is being turned by oncoming air flow moving through the rotor disk.

In this paper, we first discuss the principles of the autogyro. Next, we summarize the blade element theory of the autogyro originally presented in [12]. Subsequently, we discuss a possible method of using an autogyro-based aircraft to extract power from high altitude winds. We then use this preliminary model to investigate the feasibility of using autogyro rotors as a viable method of generating wind power through simulations. Next, we discuss future work as a result of our findings. Finally, we draw conclusions, provide acknowledgements and list references.

THE PRINCIPLES OF AUTOGYRO

An autogyro, while similar to a helicopter, has different actuation architecture and added degrees of freedom. It is comprised of three or four blades that are free to spin about their common axis; and each blade is additionally free to rotate (flap) up and down about a hinge at its root, which is normal to the spin axis. The motivation behind using the autogyro principle for energy extraction is primarily derived from the autogyro rotor being able to spin freely in wind fields and provide a substantial amount of life and torque. Since wind speeds at high altitudes are very large, an autogyro can potentially generate electricity while the lift is used to support the weight of the complete system, including the tether.

BLADE ELEMENT THEORY OF THE AUTOGYRO

A schematic diagram of a single rotor autogyro with associated forces is shown in Fig.1. Mathematical modeling of the autogyro by Glauert [12] uses the Blade Element Theory. Fig.1(a) gives a side view of the rotor. The approach is used to derive the main components, namely the thrust force T, the longitudinal force H, and the rotor torque Q. The disk of rotation of the rotor makes an angle θ with the horizontal and it is translating with a forward speed V in still air, Fig.1(a). This initial work assumes that the coning angle of a blade β is a periodic function of the blade's angular position ψ ($\dot{\psi} = \Omega$), but considers only the first harmonics, i.e.

$$\beta = \beta_0 - \beta_1 \cos(\psi - \phi_1) \tag{1}$$

This coning angle is due to the flapping DOF of each blade, as shown in Fig.1(b).

Thrust Force T

The resulting thrust force T is derived starting from a blade element located at a radial distance r along the blade, illustrated in Figs.2(a), (b) and (c). The elemental forces are then integrated over each blade span. Similar approach is taken for determining the longitudinal force H and the aerodynamic torque Q. In the aforementioned studies, expressions of steady-state T, Q and H are derived under the following assumptions:

1. The angles β and ϕ_r, shown in Figs.2(b) and (c), are small.
2. *Interference/Induced Flow*: In the vicinity of the rotor, the rotor forces generate local induced velocities which alter the undisturbed flow [12, 14]. The net effect is modeled as an

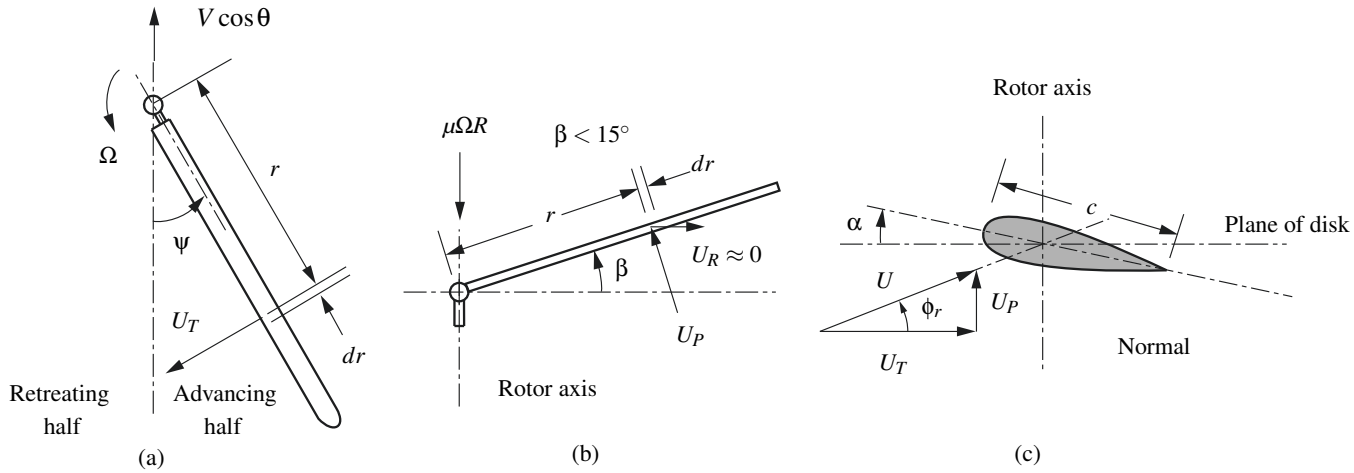

Figure 2. VELOCITIES OF A BLADE ELEMENT: (A) VIEW ALONG THE SPIN AXIS, (B) VIEW OF FLAPPING MOTION, (C) CROSS-SECTIONAL VIEW

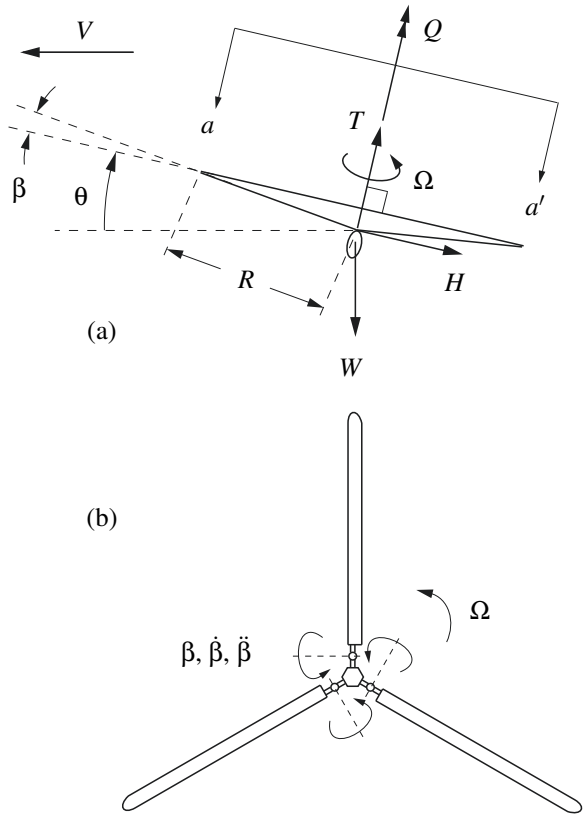

Figure 1. (A) FORCES ON AN AUTOGYRO, (B) A THREE-BLADE ROTOR VIEWED FROM PLANE aa'

induced axial velocity v

$$v = T/\left(2\pi R^2 \rho V'\right), \quad V' = \left((V\sin\theta - v)^2 + V^2\cos^2\theta\right)^{1/2} \tag{2}$$

where v modifies the effective axial velocity of wind to

$$u = V\sin\theta - v \tag{3}$$

In [12], v is assumed constant over the entire span R.

3. The lift coefficient of a blade element is proportional to $\alpha_r = \alpha + \phi_r$, *i.e.*, $C_L = k\alpha_r$, and the drag coefficient is constant, $C_D = \delta$.

Under the above conditions, the thrust is computed as

$$T = \frac{B}{2\pi}\int_0^{2\pi} d\psi \int_0^R \frac{1}{2}\rho c C_L U^2 dr \tag{4}$$

where B is the number of blades, c is the blade chord length (assumed constant), $C_L = k\alpha_r = k(\alpha+\phi_r)$ is the lift coefficient, and U is the resultant relative velocity of the wind at the element. In Eq.(4), the thrust component contributed by drag is assumed to be negligible. Assuming that the radial velocity $U_R \approx 0$, the net wind velocity U relative to a blade element is

$$\begin{aligned} U &= \sqrt{U_p^2 + U_T^2} \\ U_P &= U\sin\phi_r = u - r\dot{\beta} - (\beta+\chi)V\cos\theta\cos\psi \\ U_T &= U\cos\phi_r = \Omega r + V\cos\theta\sin\psi \end{aligned} \tag{5}$$

where u is defined in Eq.(3), β is assumed to be a function of ψ as in Eq.(1), and χ is a geometric property of the airfoil sections of each blade, [12]. The Eq.(5) can be expressed as

$$\begin{aligned} U\sin\phi_r &= \mu\Omega R - \Omega r\beta_1\sin(\psi-\psi_1) - (\beta_0+\chi)V\cos\theta\cos\psi \\ U\cos\phi_r &= \Omega r + V\cos\theta\sin\psi \end{aligned} \tag{6}$$

For the autogyro, we define the following two speed ratios:

$$\lambda = \frac{V}{\Omega R}, \quad \mu = \frac{u}{\Omega R}. \tag{7}$$

The first speed ratio, λ, is the tip-speed ratio. The second, μ, represents the inflow ratio of wind passing through the rotor disk. Assuming ϕ_r to be small, as well as observing that the periodic terms appearing in U_T and U_P in Eq.(5) would cancel when the B equispaced blades are taken into consideration,

$$\sum_{i=1}^{B} \sin\left(\psi + \frac{2\pi}{B}(i-1)\right) = \sum_{i=1}^{B} \cos\left(\psi + \frac{2\pi}{B}(i-1)\right) = 0 \quad (8)$$

we obtain the approximation

$$\phi_r \approx \tan\phi_r = \frac{\mu R}{r} \quad (9)$$

Since the above approximations break down towards the root of each blade and over a wider span of the blades in the retreating half (see Fig.2(a)), the following two conditions are imposed under which the calculated force T will be representative of the physical phenomena.

1. U_T must be positive over the outer half of the retreating blades, implying from Eq.(5), $V\cos\theta < 0.5\Omega R$.
2. The outer half of each blade operates below a critical angle, *i.e.* $\alpha_r = \alpha + \phi_r < \alpha_{cr}$ for $0.5R \le r \le R$ and for all $\psi \in [0,\ 2\pi]$.

Under these conditions, the expression in Eq.(4) evaluates to

$$T = T_c \pi \rho \Omega^2 R^4, \quad T_c = \sigma\left(\alpha + \frac{3}{2}\mu\right) \quad (10)$$

where $\sigma = Bc/\pi R$ is the blade solidity.

Aerodynamic Torque Q

The average aerodynamic torque generated over one complete rotation for B blades, and using the assumptions listed above, is

$$Q = \frac{B}{2\pi}\int_0^{2\pi} d\psi \left[\int_0^R \frac{1}{2}\rho c\left(C_L U^2 \sin\phi_r - C_D U^2\right) r dr\right] \quad (11)$$

Upon carrying out the integration, and using Eqs.(8) and (10), Q reduces to

$$Q = Q_c \pi R^2 \rho \Omega^2 R^3, \quad Q_c = \frac{1}{4}\sigma\delta - \mu T_c \quad (12)$$

where $C_D = \delta$ is a constant drag coefficient assumed for low angles of attack. Under steady-state operation, let the autogyro provide a thrust force $T = W_d$, where $W_d > W$, with W being the total weight to be supported. Then, setting $Q = 0$ and noting that a sensible solution has $\mu > 0$, from Eqs.(10), (11), and (12) we find the following expressions for steady-state μ and spin speed Ω

$$\mu = \frac{1}{3}\left[\sqrt{\alpha^2 + \frac{3}{2}\delta} - \alpha\right], \quad \Omega = \sqrt{\frac{W_d}{Bc\rho R^3(\alpha + \frac{3}{2}\mu)}} \quad (13)$$

Longitudinal and Lateral Forces

The longitudal force is similarly obtained by integrating over blade elements. The final expression is $H = H_c \pi R^2 \rho \Omega^2 R^2$, where H_c is a function of σ, α, μ, λ, θ and geometric parameters of the blade. A lateral force Y is also generated (perpendicular to the plane of the paper in Fig.1(a)) due to differences in aerodynamic forces between the advancing half and the retreating half. This force is of secondary importance and the detailed derivation of Y and H can be found in [12]. Both derivations of Y and H involve the equation of motion of flapping of each blade, which has the general form

$$I_1\left(\ddot{\beta} + \Omega^2\beta\right) = TM_1 - G_1 - \Omega^2 J_1 \quad (14)$$

where, the subscipt (1) denotes values for a single blade, TM denotes the flapping moment due to thrust force, G_1, I_1 and J_1 are line integrals involving line density m (assumed constant) of the blade and are dependent on the blade geometry. Specifically,

$$G_1 = \int_0^L mgrdl, \quad I_1 = \int_0^L mr^2 dl, \quad J_1 = \int_0^L mh(r)rdl \quad (15)$$

where, $h(r)$ is a geometric parameter and L is the length of each blade (Note: L is not necessarily equal to R).

Lift and Drag Formulation

The cummulative lift and drag forces generated by the autogyro are related to the thrust T and longitudinal force H through the relations

$$\begin{aligned} F_L &= (T\cos\theta - H\sin\theta) = k_L \pi R^2 \rho V^2 \\ F_D &= (T\sin\theta + H\cos\theta) = k_D \pi R^2 \rho V^2 \end{aligned} \quad (16)$$

where k_L, k_D are the lift and drag coefficients. They are related to the coefficient of thrust T_c and the coefficient of longitudinal force H_c through the relation

$$k_L = \frac{T_c\cos\theta - H_c\sin\theta}{\lambda^2} \quad (17)$$

$$k_D = \frac{T_c\sin\theta + H_c\sin\theta}{\lambda^2} \quad (18)$$

T_c is defined in Eq.(10) and λ is the tip-speed ratio defined in Eq.(7).

Table 1. SIMULATION PARAMETERS

Parameter	Value	Description
B	4	Number of blades
R	17.5	Blade radius (ft)
W	1500	Total weight of autogyro (lbs.)
c	2.75	Blade chord (ft)
σ	$\frac{Bc}{\pi R}$	Rotor solidity
δ	0.006	Mean airfoil drag coefficient
α	0.035	Blade pitch angle (radians)
ρ	0.0008	Air density at 10km altitude (slugs/ft^3)

AUTOGYROS FOR ENERGY HARVESTING

For energy extraction, we consider V to be the steady horizontal wind speed instead of the steady aircraft speed in still air. Energy extraction using a generator effectively provides a load torque Q_e and reduces the steady state angular velocity Ω. Incorporating Q_e in the analysis amounts to simply setting $Q = Q_e$ in Eq.(12) instead of setting $Q = 0$. This results in

$$1.5W_dR\mu^2 + (W_dR\alpha - 1.5Q_e)\mu - (Q_e\alpha + 0.25W_dR\delta) = 0 \quad (19)$$

which is solved for μ, while the steady-state Ω retains the same expression in Eq.(13).

SIMULATION RESULTS

The steady-state model of the autogyro discussed above was used to compute the lift and drag coefficients, the lift and drag forces, and the relative velocity of the wind for autogyro operation, all as a function of the angle of incidence θ. The parameter values used are similar to those in [14], for which experimental validation was done. The rotor was assumed to have four blades and each blade was assumed to have a length of 17.5 ft and weigh 3% of the total weight of the aircraft. Other parameter values of the simulation are provided in Table 1. The value for the density of air was chosen in order to simulate high altitude operation. US units were chosen for comparing results with published results. The following sequence can be used to carry-out the steady-state calculations:

1. Choose a target thrust force $W_d > W$ and a given load torque Q_e.
2. Choose a suitable range of values of $\tau = \lambda\cos\theta$.
3. Solve for μ from Eq.(19), and Ω from Eq.(13).
4. Solve for T_c and H_c. T_c is given in Eq.(10) and H_c can be found from [12].
5. From Eqs.(2), (3), (7) and (10) we can show that:

$$\lambda\sin\theta = \mu + \frac{\frac{1}{2}T_c}{\sqrt{\mu^2 + \lambda^2\cos^2\theta}} \quad (20)$$

   Solve for $\lambda\sin\theta$ for each value of $\lambda\cos\theta$.
6. Solve for λ, θ, and solve for V.
7. Solve for k_L, k_D and F_L and F_D.

To validate the model against results given in [12], an initial set of simulations was done for $Q_e = 0$. This can be considered as pure autogyro mode of operation where there is no load torque. The results are shown in Figs.3 (a), (b), (c). For a target lift force of $W = 1500$ lb, the target thrust force of $W_d = 2000$ lb was chosen Figure 3(a) verifies the condition $V\cos\theta < 0.5\Omega R$, illustrating that the condition is violated only for a small range of incidence angles $\theta < 5^\circ$. Figure 3(b) indicates that the target lift force of $W = 1500$lbs will be achievable for $\theta \leq 40^\circ$. Figure 3(c) plots the steady-state relative velocity of the wind that will generate the thrust W_d for a desired angle of incidence θ.

In the investigation above, 88% of the lift supports the weight of the aircraft (the blades weigh only 12% of the total weight). For an inertially fixed autogyro in a wind field, the lift will be reduced since the autogyro will drive a generator. In addition to the weight of the aircraft, the autogyro rotors will have to support the weight as well as the force of drag on a tether. Preliminary calculations, performed with a 5 mm diameter K-49 Kevlar cable [9] indicates that this force will be much less than the weight W.

The effect of energy extraction is next studied by simulating with various values of Q_e. Results with $Q_e = 1000$lb.ft are shown in Figs.3(d), (e), (f). As expected, power extraction results in (i) reduced value of k_L, (ii) violation of the condition $V\cos\theta < 0.5\Omega R$ over a greater range of θ, and (iii) increase in the required wind velocity to generate the same W_d. From the results, it is evident that an effective lift force is generated with $20^\circ \leq \theta \leq 40^\circ$, and higher values of θ is better suited for lowering V.

Next we investigate the validity of the results against underlying assumptions of this theory. As mentioned earlier, the theory is considered valid under two conditions, namely

1. U_T must be positive over the outer half of the retreating blades, implying from Eq.(5), $V\cos\theta < 0.5\Omega R$.
2. The outer half of each blade operates below a critical angle, *i.e.* $\alpha_r = \alpha + \phi_r < \alpha_{cr}$ for $0.5R \leq r \leq R$ and for all $\psi \in [0,\ 2\pi]$.

The first condition, checked using Figs.3 (a) and (d) for $Q_e = 0$ and $Q_e = 1000$ lb.ft, is not too restrictive. The main constraint on the model's accuracy appears to be the second condition. To verify the validity of this condition, the small angle assumption

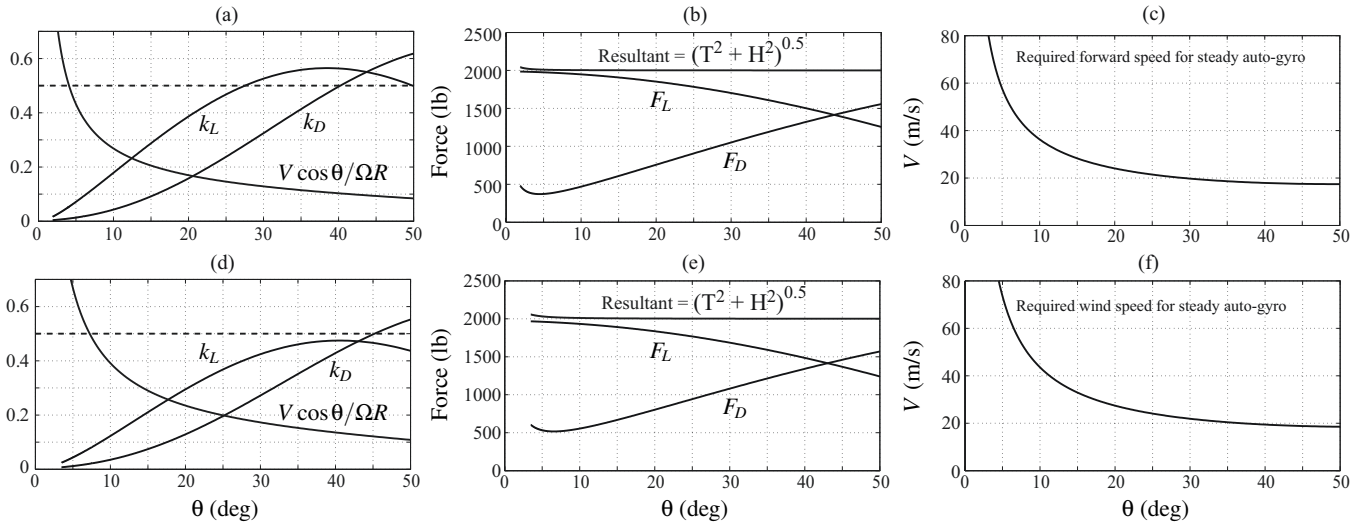

Figure 3. STEADY-STATE OPERATION OF A SINGLE AUTOGYRO WITH VARYING ANLGES OF INCIDENCE. SUBFIGURES (A), (B), (C) CORRESPOND TO $Q_e = 0$, SUBFIGURES (D), (E), (F) CORRESPOND TO $Q_e = 1000$ LB·FT.

on ϕ_r was removed and the complete expression for ϕ_r, namely

$$\tan\phi_r = \frac{\Omega R\mu - \Omega r\beta_1 \sin(\psi - \phi_1) - [\beta_0 + \chi(r)]\, V\cos\theta\cos\psi}{\Omega r + V\cos\theta\sin\psi} \tag{21}$$

was maximized over one full rotation of a blade $\psi \in [0, 2\pi]$. The maximum ϕ_r was used to calculate the maximum angle of attack using the relation $\alpha_r = \alpha + \phi_r$, as a function of $r \in [0, R]$. The maxima were plotted for generator torques $Q_e = 0$ and $Q_e = 1000$ lb·ft; the results are shown in Figs.4(a) and (b). For the targeted range of incidence angle $\theta \in [20^\circ, 40^\circ]$, it can be seen that while stall angles of $\alpha_{cr} \geq 9^\circ$ would be sufficient when $Q_e = 0$, the stall angle requirement increases to $\alpha_{cr} \geq 11^\circ$ when $Q_e = 1000$. This is expected since power extraction leads to a load torque that reduces Ω.

Finally, using the expression in Eq.(13) for average Ω, the power extraction from the autogyro was calculated for a range of Q_e values. The results are shown in Fig.5. Figure 5(a) shows the mechanical power extracted and Figure 5(b) shows the steady-state rotor speed needed to maintain sufficient lift as a function of generator torque Q_e.

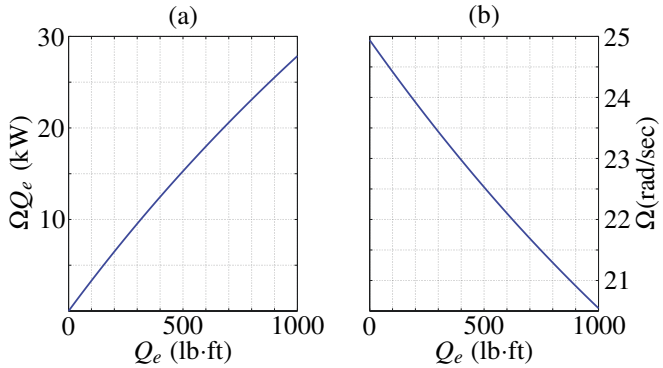

Figure 5. (A) POWER EXTRACTED (B) STEADY STATE Ω NEEDED TO MAINTAIN REQUIRED LIFT

MODEL REFINEMENT AND FUTURE WORK

The analysis presented is a good start, but there are assumptions in the underlying theory which can be relaxed. The first work on autogyro modeling [12] uses the blade element theory approach [15] to derive the thrust force T, the longitudinal force H, and the rotor torque Q. [13] extended this work by relaxing one of the main assumptions, that the squares and higher powers of the ratio of the forward speed to the tip speed τ are negligible. To this end, [13, 14] show that terms of the order of τ^4 can be incorporated in formulations of T, H, and Q if the Fourier expansion of β in terms of ψ includes second-order harmonics, *i.e.*,

$$\beta = \beta_0 - \beta_1\cos(\psi - \phi_1) - \beta_2\cos(2(\psi - \phi_2)) \tag{22}$$

where ϕ_1 and ϕ_2 are arbitrary constants. The extension in [13] showed a lift-to-drag ratio higher than that predicted in [12].

Wheatley, [14], extended the work in [12, 13] by considering blades with pitch varying along their span. This was an effort to validate experimental data obtained from the Pitcairn-Cierva autogyro, one of the first functional autogyros [16] The work also incorporated a detailed analysis of the forces in the retreating half of the rotor, Figure 2(a), where the blade velocities are reversed. A variant of the autogyro design, better known as the gyroplane, was also studied in [17]. In contrast to the autogyro, where each blade can flap independently, a gyroplane has an even number of blades; the opposite blades are rigidly connected and are allowed

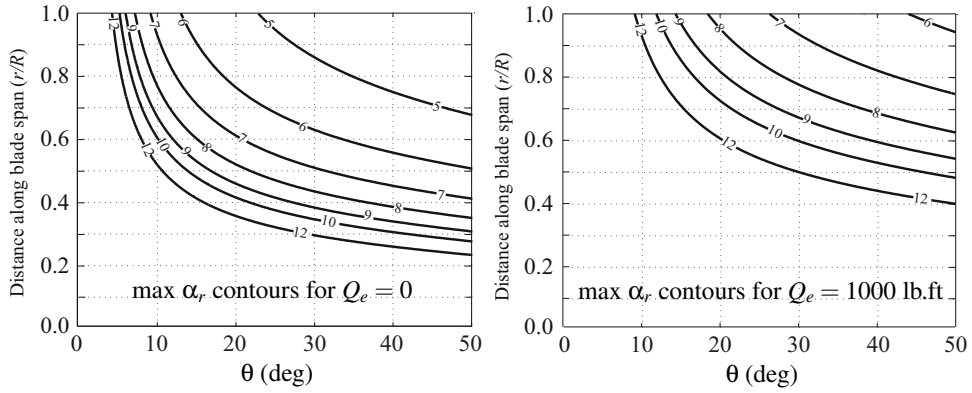

Figure 4. MAXIMUM ANGLE OF ATTACK α_r ALONG THE BLADE SPAN OVER ONE COMPLETE ROTATION

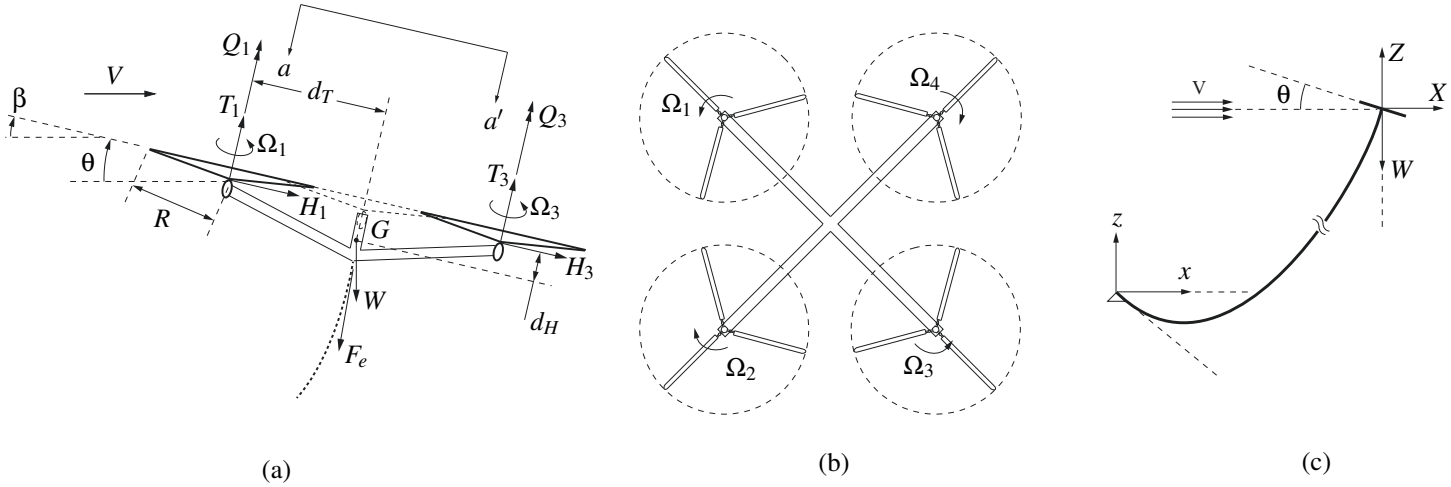

Figure 6. CONCEPT OF AN AUTOGYRO-BASED QUADROTOR FOR ENERGY HARVESTING (A) FORCES ON A TETHERED AUTOGYRO QUADROTOR, (B) VIEW OF THE QUADROTOR FROM PLANE aa', (C) GLOBAL VIEW OF SIMPLIFIED AUTOGYRO-BASED AIRBORNE WIND ENERGY DEVICE

to feather, *i.e.*, freely rotate about their span axis. Although the gyroplane is structurally different from the autogyro, both have additional d.o.f. when compared to wind turbines and analytical results in [17] indicate that they have similar overall lift coefficients and lift-to-drag ratios. Other extensions include [18], which models the effect of twisting of blades due to aerodynamic forces, and [19] which refines the analysis in the retreating half for larger angles of attack and higher speeds.

An interesting area of potential research with this concept would be maneuverability and atitude control of the entire power generation system. In Figure 6, we describe a potential configuration of the autogyro rotors in the form of a quadropter. The quadropter configuration poses an interesting controls problem from the standpoint of transitioning from powered flight to an autogyro mode, as well as performing various positioning and orientation maneuvers. Our future work will include addressing this problems using theoretical analysis, computer simulations, and physical experiments.

ACKNOWLEDGEMENT

The authors thank Professor Ranjan Mukherjee of Michigan State University for his insightful comments and advice in the technical development of this research.

CONCLUSION

We have provided some preliminary results which support the potential feasibility of using an autogyro-based tethered device for high altitude wind energy harvesting. A model of a single autogyro was developed based on past work by Glauert [12] where the main focus was aviation, rather than energy harvesting. For addressing the latter, the effect of wind energy extraction was modeled as an additional braking torque. Steady-state conditions were computed to estimate the operating incidence angles and prevailing wind speeds needed for steady autogyro operation while extracting power. While initial impressions indicate that such a device could work, additional research needs to be carried out in order to further validate the concept.

REFERENCES

[1] Archer, C. L., and Caldiera, K., 2009. "Global assessment of high-altitude wind power". In Energies, Vol. 2, pp. 307–319.

[2] Roberts, B. W., Shepard, D. H., Caldiera, K., Cannon, M. E., Eccles, D. G., Grenier, A. J., and Freidin, J. F., 2007. "Harnessing high-altitude wind power". In IEEE Transactions on Energy Conversion, Vol. 22, pp. 136–144.

[3] Manalis, M. S., 1975. "Airborne windmills: Energy source for communication aerostats". In AIAA Lighter Than Air Technology Conference.

[4] Fletcher, C. A. J., 1979. "On the rotary wing concept for jet stream electricity generation". In Journal of Energy.

[5] Ockels, W. J., 2001. "Laddermill, a novel concept to exploit the energy in the airspace". In Aircraft Design.

[6] Williams, P., Lansdorp, B., and Ockels, W. J., 2007. "Modeling and control of a kite on a variable length inelastic tether". In AIAA Modeling and Simulation Technologies Conference and Exhibit.

[7] Williams, P., Lansdorp, B., and Ockels, W. J., 2008. "Optimal cross-wind towing and power generation with tethered kites". In AIAA Journal of Guidance, Control, and Dynamics.

[8] Williams, P., Lansdorp, B., and Ockels, W. J., 2008. "Nonlinear control and estimation of a tethered kite in changing wind conditions". In AIAA Journal of Guidance, Control, and Dynamics.

[9] Garcia-Sanz, M., and Houpis, C. H., 2012. *Wind Energy Systems: Control Engineering Design*. CRC Press.

[10] Rimkus, S., Das, T., and Mukherjee, R., 2013. "Stability analysis of a tethered airfoil". In American Controls Conference.

[11] Das, T., Mukherjee, R., Sridhar, R., and Hellum, A., 2011. "Two-dimensional modeling and simulation of a tethered airfoil system for harnessing wind energy". In ASME Dynamic Systems and Control Conference.

[12] Glauert, H., 1926. A general theory of the autogyro. Tech. rep., Aeronautical Research Council.

[13] Lock, C. N. H., 1927. Further development of autogyro theory, part i. Tech. rep., Aeronautical Research Council.

[14] Wheatley, J. B., 1934. An aerodynamic analysis of the autogiro rotor with a comparison between calculated and experimental results. 487, National Advisory Committee for Aeronautics.

[15] Gessow, A., and Myers, G. C., 1952. *Aerodynamics of the Helicopter*. Macmillan Company.

[16] Charnov, B. H., 2003. *From Autogyro to Gyroplane: The Amazing Survival of an Aviation Technology*. Praeger Publishers.

[17] Wheatley, J. B., 1934. The aerodynamic analysis of the gyroplane rotating-wing system. Tech. Rep. 492, National Advisory Committee for Aeronautics.

[18] Wheatley, J. B., 1937. An analytical and experimental study of the effect of periodic blade twist on the thrust, torque, and flapping motion of an autogyro rotor. Tech. Rep. 591, National Advisory Committee for Aeronautics.

[19] Gessow, A., and Crim, A. D., 1952. An extension of lifting rotor theory to cover operation at large angles of attack and high inflow conditions. Tech. rep., National Advisory Committee for Aeronautics.